Research Square

Preprints are preliminary reports that have not undergone peer review.
They should not be considered conclusive, used to inform clinical practice,
or referenced by the media as validated information.

Metabolic decoupling of growth and hydrolytic enzyme production in Bacillus amyloliquefaciens SLBD under different carbon sources

Epi Taufik

epitaufik@apps.ipb.ac.id

IPB University

Rifqi Hafidz Ash Shiddiq

IPB University

Haslina Asis

University Malaysia Sabah

Muhamad Arifin

IPB University

Slamet Widodo

IPB University

Huda Shalahudin Darusman

IPB University

Rafida Raazali

Universiti Malaysia Sarawak

Cahyo Budiman

IPB University

Research Article

Keywords: Bacillus amyloliquefaciens SLBD, Growth Media, Protease, Lipease, Cellulases

Posted Date: August 20th, 2026

DOI: https://doi.org/10.21203/rs.3.rs-10644538/v1

License: This work is licensed under a Creative Commons Attribution 4.0 International License.
Read Full License

Additional Declarations: No competing interests reported.

Abstract

This study investigates the influence of different carbon sources on the growth kinetics and extracellular hydrolytic enzyme production of *Bacillus amyloliquefaciens* SLBD, with a focus on protease, lipase, and cellulase as representative enzymes targeting proteins, lipids, and carbohydrates. Batch cultivation was conducted using glycerol, D-glucose, sucrose, D-fructose, maltose, and inulin hydrolysate as sole carbon sources. Growth behavior was monitored through OD_{600} measurements, while enzyme activities were quantified using substrate-specific spectrophotometric assays. The results demonstrated that carbon source selection significantly affects both bacterial growth and enzyme secretion. Glycerol supported the highest specific growth rate ($\mu = 0.225\ h^{-1}$) and biomass accumulation, indicating efficient metabolism with minimal carbon catabolite repression (CCR). In contrast, glucose promoted rapid early growth but limited enzyme production due to CCR effects. Enzyme production was strongly growth phase-dependent, with maximal activities observed during the late exponential to early stationary phase. Protease and lipase activities were highest in glycerol-grown cultures, while cellulase activity peaked in media supplemented with inulin hydrolysate, reflecting induction by complex substrates. Partial purification using stepwise ammonium sulfate precipitation followed by size exclusion chromatography enabled selective enrichment of the three enzymes from a single extracellular fraction, with distinct precipitation profiles at 60%, 80%, and 90% saturation for protease, cellulase, and lipase, respectively. SDS–PAGE analysis confirmed molecular weights of approximately 35 kDa (protease), 56 kDa (lipase), and 70 kDa (cellulase), although complete purity was not achieved. Overall, this study highlights the interplay between carbon metabolism, growth dynamics, and enzyme production, providing insights for optimizing cost-effective multi-enzyme production systems from locally sourced bacterial strains.

Introduction

Hydrolytic enzymes represent a major class of biocatalysts with extensive industrial and biotechnological applications, owing to their ability to catalyze the breakdown of complex macromolecules into simpler, value-added products (Wang et al. 2024). Among these, proteases, lipases, and cellulases are particularly significant, collectively contributing to a substantial proportion of the global enzyme market due to their versatility across sectors such as food processing, agriculture, pharmaceuticals, detergents, and waste valorization (Adeoyo 2025). Proteases catalyze the hydrolysis of peptide bonds in proteins, enhancing protein digestibility and nutrient availability in livestock systems (Razali et al. 2021; Razali et al. 2020). Lipases hydrolyze triglycerides into fatty acids and glycerol, playing essential roles in lipid metabolism, biodiesel production, and food modification processes (Yahya et al. 2025). Meanwhile, cellulases degrade cellulose into fermentable sugars, forming the backbone of lignocellulosic biomass conversion and bioenergy production (Obeng et al. 2017). The combined study of these three enzymes therefore provides a representative model of microbial hydrolytic capacity toward proteins, lipids, and carbohydrates—the three major classes of biological macromolecules.

In livestock and agro-industrial contexts, the coordinated action of these hydrolytic enzymes is particularly important for improving feed efficiency, nutrient cycling, and waste bioconversion, thereby

supporting sustainable production system (Imran et al. 2016). However, many developing countries still depend heavily on imported enzyme preparations, leading to increased production costs and limited technological autonomy (Astuti et al. 2024). This highlights the urgent need to explore and optimize local microbial resources capable of producing multiple hydrolytic enzymes efficiently under cost-effective fermentation conditions.

Among microbial producers, bacteria from the genus Bacillus are well known for their ability to secrete a broad spectrum of extracellular hydrolytic enzymes with high stability and catalytic efficiency (Kumar et al. 2024). Importantly, the production of these enzymes is not constitutive but tightly regulated by environmental and nutritional factors. Among these, the nature of the carbon source plays a central role, as it governs cellular metabolism, growth kinetics, and the allocation of metabolic resources toward either biomass formation or enzyme secretion (Ma et al. 2024). Consequently, the selection of an appropriate carbon substrate becomes a key determinant in optimizing fermentation strategies for enhanced hydrolytic enzyme production.

Carbon sources can exert both stimulatory and inhibitory effects on enzyme biosynthesis through regulatory mechanisms such as carbon catabolite repression (CCR) (Sonnleitner 2025). Readily metabolizable sugars such as D-glucose and D-fructose, often support rapid cell growth but may repress the synthesis of extracellular enzymes, including proteases, lipases, and cellulases, as cells prioritize energy-efficient metabolic pathways (Kognou et al. 2023). In contrast, more complex carbohydrates or alternative substrates—such as sucrose, maltose, glycerol, and inulin hydrolysate—may relieve CCR and promote enzyme secretion by shifting metabolism toward substrate scavenging and extracellular degradation (Meng et al. 2026). This metabolic transition is typically associated with the late exponential or stationary growth phases, where hydrolytic enzyme production often reaches its maximum. Therefore, understanding the interplay between carbon source utilization, growth dynamics, and enzyme expression is essential to balance biomass accumulation with enzyme yield (Ma et al. 2024).

In this context, *Bacillus amyloliquefaciens* SLBD, isolated from animal feces, represents a promising model organism for investigating carbon-dependent hydrolytic enzyme production. The fecal environment is inherently rich in complex organic matter, exerting selective pressure on resident microorganisms to develop diverse enzymatic systems for efficient nutrient degradation (Korajkic et al. 2019). Previous studies have demonstrated strong cellulolytic activity in this strain, while genomic analysis has revealed multiple genes encoding putative proteases and lipases (Shiddiq et al. 2025). These characteristics suggest that *B. amyloliquefaciens* SLBD possesses metabolic versatility, enabling differential responses to various carbon substrates that may influence both growth performance and multi-enzyme secretion profiles.

Despite this potential, the relationship between carbon source utilization, bacterial growth kinetics, and the production of key hydrolytic enzymes in this strain remains insufficiently understood. Therefore, this study aims to systematically evaluate the effects of different carbon sources—glycerol, D-glucose, sucrose, D-fructose, maltose, and inulin hydrolysate—on the growth behavior of *B. amyloliquefaciens*

SLBD and to elucidate their influence on the production of extracellular hydrolytic enzymes, using protease, lipase, and cellulase as representative models. By integrating growth and enzyme production data, this work seeks to provide fundamental insights into metabolic regulation and to support the development of efficient and economically viable strategies for multi-enzyme production in industrial applications

Material and methods

Bacterial strain

The bacterial strain used in this study was *Bacillus amyloliquefaciens* SLBD, previously isolated from fresh animal feces and characterized based on morphological, physiological, biochemical properties, and 16S rRNA gene sequence analysis (Shiddiq et al. 2025). The strain was maintained in 20% (v/v) glycerol stocks at −80 °C.

Medium preparation and inoculum development

All chemicals used were of analytical grade. The maintenance medium consisted of (g L^{-1}): D-glucose 20, peptone 5, beef extract 5, $Na_2HPO_4 \cdot 12H_2O$ 1, citric acid 1, $CaCO_3$ 10, and agar 20, adjusted to pH 6.5 prior to sterilization. For inoculum preparation, a single colony from a freshly streaked agar plate was transferred into 100 mL of seed medium in a 500 mL Erlenmeyer flask. The seed medium contained (g L^{-1}): D-glucose 20, peptone 5, beef extract 5, $Na_2HPO_4 \cdot 12H_2O$ 5, and citric acid 1. The culture was incubated at 30 °C with shaking at 160 rpm for 18–24 h until reaching the mid-exponential phase (OD_{600} ≈ 0.8–1.0).

Cultivation under different carbon sources

To evaluate the effect of carbon sources on bacterial growth, method of Lindang et al. 2021 was used with modifications, in which batch cultures were performed using a defined basal medium containing (g L^{-1}): beef extract 8 and ethanol 14, with the pH adjusted to 6.5. The carbon source was varied by supplementing the medium with 50 g L^{-1} of one of the following substrates: glycerol, D-glucose, sucrose, D-fructose, maltose, or inulin hydrolysate. A 2% (v/v) inoculum from the seed culture was transferred into 100 mL of sterilized medium in 500 mL flasks. Cultures were incubated at 37 °C.

Growth curve determination

Bacterial growth was monitored by measuring optical density at 600 nm (OD_{600}) at certain interval throughout the cultivation period (Yahya et al. 2025, Lindang et al. 2021). Samples (1 mL) were aseptically withdrawn, and OD_{600} was measured using a UV–Vis spectrophotometer against a sterile medium blank. To improve accuracy at high cell densities, samples exceeding OD_{600} > 0.8 were appropriately diluted with sterile saline solution prior to measurement. Growth curves were constructed by plotting OD_{600} against cultivation time to determine key growth phases, including lag, exponential,

stationary, and decline phases. Each experiment was conducted in triplicate, and the results were expressed as mean ± standard deviation.

Determination of specific growth rate (μ)

The specific growth rate (μ) was determined according to Hall et al. 2014, based on optical density (OD_{600}) measurements obtained during batch cultivation. Growth curves were constructed by plotting OD_{600} values against incubation time. To estimate μ, the exponential growth phase for each condition was first identified from the semi-logarithmic plot of ln (OD_{600}) versus time, where a linear relationship indicates exponential cell growth. The specific growth rate (μ, h^{-1}) was calculated using the following equation:

$$\mu = \frac{\ln X_2 - \ln X_1}{t_2 - t_1} \quad (1)$$

where X1 and X2 represent the optical density values (OD_{600}) at time points $t1$ and $t2$, respectively, within the exponential growth phase. For each carbon source, at least two time points within the linear region of the ln (OD_{600}) plot were selected to calculate μ. In addition, linear regression analysis of ln (OD_{600}) versus time was performed to confirm the consistency of the exponential phase, and the slope of the fitted line was taken as the specific growth rate.

Extracelular fraction (EF) collection during growth course

Extracellular fractions (EF) were collected, according to Yahya et al. 2025, throughout the bacterial growth course to monitor enzyme production dynamics. At each sampling time point corresponding to OD_{600} measurements, culture aliquots were withdrawn and centrifuged at 8,000 × g for 15 min at room temperature. The resulting supernatants were carefully collected and subsequently filtered through a 0.22 μm membrane to remove any residual cells, yielding cell-free extracellular fractions. These EF samples, corresponding to each incubation time, were used for subsequent determination of protein concentration and enzymatic activity profiles.

Determination of protein concentration

Protein concentration of the extracellular fractions was determined using the Lowry method, with bovine serum albumin (BSA) as the standard (Vershinina et al. 2025). Briefly, appropriately diluted samples were reacted with alkaline copper reagent followed by Folin–Ciocalteu reagent, and the absorbance was measured at 750 nm. Protein concentrations were calculated from a standard calibration curve constructed using BSA.

Proteolytic activity assay

Proteolytic activity was determined using the chromogenic substrate N-succinyl-Ala-Ala-Pro-Phe-p-nitroanilide (Suc-AAPF-pNA), following the method described by Falkenberg et al. 2022 with slight modifications. The assay was performed at 30 °C in 100 mM Tris–HCl buffer (pH 8.0). A stock solution of Suc-AAPF-pNA (110 mM) was prepared in dimethyl sulfoxide (DMSO) and diluted 1:100 in the reaction mixture prior to use. The reaction was initiated by adding an appropriate volume of enzyme sample to the substrate solution. The release of p-nitroaniline was monitored spectrophotometrically at 410 nm, with absorbance recorded every 30 s for 5 min using either a UV–Vis spectrophotometer (1 mL cuvette) or a microplate reader (250 µL format). The concentration of released product was calculated using the molar extinction coefficient of p-nitroaniline (ε_{410} = 8.48 $mM^{-1}{\cdot}cm^{-1}$). One unit (U) of protease activity was defined as the amount of enzyme required to release 1 µmol of p-nitroaniline per minute under the assay conditions. Specific activity was expressed as U mg^{-1} protein.

Lipolytic activity assay

Lipase activity was measured according to Yahya et al. 2025 using p-nitrophenyl palmitate (pNPP) as the substrate. Briefly, solution A was prepared by dissolving 1 mg of pNPP in 1 mL isopropanol. This was subsequently added to solution B containing 0.01 g gum arabic, 0.02 g sodium deoxycholate, 50 µL Triton X-100, and 9 mL of 50 mM Tris–HCl buffer (pH 8.0). The reaction mixture consisted of 700 µL pNPP solution and 300 µL enzyme sample in a 1 mL cuvette. The release of p-nitrophenol was monitored at 410 nm during the initial 2 min of reaction. One unit (U) of lipase activity was defined as the amount of enzyme releasing 1 µmol of p-nitrophenol per minute under the assay conditions (ε = 1500 $L{\cdot}mol^{-1}{\cdot}cm^{-1}$).

CMC cellulolytic activity assay

Carboxymethyl cellulase (CMCase) activity was determined using carboxymethyl cellulose (CMC) as substrate. The reaction mixture consisted of 50 µL enzyme sample and 50 µL of 1% (w/v) CMC prepared in 100 mM phosphate buffer (pH 7.0). The mixture was incubated at 50 °C for 20 min. The reaction was terminated by adding 0.3 mL of 3,5-dinitrosalicylic acid (DNS) reagent, followed by heating in boiling water for 5 min to develop color. Absorbance was measured at 540 nm using a microplate reader, following the method of Potprommanee et al. 2017. The concentration of reducing sugars released was quantified using the DNS method described by Miller 1959. One unit (U) of cellulase activity was defined as the amount of enzyme required to release 1 µmol of glucose per minute under the assay conditions.

Partial purification of the enzymes

The culture condition exhibiting the highest enzymatic activity for each enzyme (protease, lipase, and cellulase) was selected for partial purification, according to Fathi 2021. Crude extracellular enzyme preparations were obtained from the corresponding optimal incubation time by centrifugation, as described above. Protein precipitation was first carried out using ammonium sulfate at 20-90% saturation. The mixture was incubated at 4 °C for 24 h to allow complete precipitation. The precipitated proteins were recovered by centrifugation, resuspended in 10 mM Tris–HCl buffer (pH 8.0), and dialyzed

overnight against the same buffer. The dialyzed sample was then filtered through a 0.45 µm membrane to remove residual particulates. The enzymatic activity (protease, lipase and celulases) from each concentration of salt was determined according to the assay for each enzyme. The salt concentration gave highest enzymatic activity was then used for further step of purification.

Further purification was performed using size exclusion chromatography (SEC) on a HiLoad 16/60 Superdex 200 pg column (GE Healthcare, Amersham, UK), pre-equilibrated with 50 mM Tris–HCl buffer (pH 8.0) containing 50 mM NaCl. Elution was carried out at a flow rate of 0.5 mL min^{-1}, as described previously (Budiman et al. 2022). The purity of the fractions was analyzed by 15% SDS–polyacrylamide gel electrophoresis (SDS–PAGE) following the method of Laemmli 1970. Protein concentration and enzymatic activities (protease, lipase, and CMCase) of each fraction were determined using the methods described above.

Results and Discussion

Growth curve

The growth profiles of *Bacillus amyloliquefaciens* SLBD cultivated on different carbon sources exhibited a typical sigmoidal pattern, consisting of lag, exponential, stationary, and decline phases, although the duration and intensity of each phase varied depending on the substrate (Fig. 1**).** This typical sigmoid curve was also reported for this strain when it grew under Luria-Bertani (LB) broth medium, as reported by Shiddiq et al. 2025. Across all conditions, a short lag phase was observed within the first 2–5 h, indicating rapid physiological adaptation of the strain to the provided substrates. This was followed by a clear exponential phase between approximately 5 and 15–20 h, during which cell density increased markedly. Among the tested carbon sources, D-glycerol supported the most pronounced exponential growth and reached the highest biomass accumulation, followed by D-glucose and inulin hydrolysate. In contrast, sucrose, maltose, and D-fructose resulted in comparatively slower growth and lower final cell densities. After 20–24 h, most cultures transitioned into stationary phase, with some substrates (e.g., glycerol and glucose) maintaining higher cell densities for longer periods, while others exhibited an earlier onset of decline. Lee et al. 2017 earlier reported that variation on the length of growth phase in *B. amyloliquefaciens* were typical, depending on the strain and growth condition, including the growth medium.

Comparatively, the superior growth observed in glycerol-containing medium suggests that this carbon source is efficiently metabolized by the SLBD strain, likely due to its entry into central metabolism via glycerol kinase and subsequent conversion to dihydroxyacetone phosphate (DHAP), which feeds directly into glycolysis (Zhang et al. 2022; Bizzini et al. 2010; Pan et al. 2024). Unlike glucose, glycerol metabolism is generally less associated with strong carbon catabolite repression (CCR), allowing sustained metabolic activity without significant repression of alternative metabolic pathways (Brückner and Titgemeyer 2002). This is consistent with the extended exponential phase and higher OD_{600} values observed for glycerol. In contrast, although D-glucose supported rapid initial growth, its effect plateaued

earlier, likely due to CCR mechanisms that prioritize energy-efficient pathways while repressing genes involved in the utilization of alternative substrates and secondary metabolism, as reported by Kopp et al. 2018.

The moderate growth observed with inulin hydrolysate is particularly noteworthy, as it reflects the ability of *B. amyloliquefaciens* SLBD to utilize more complex carbohydrate mixtures. Inulin hydrolysate typically contains fructooligosaccharides and fructose, which require additional enzymatic processing prior to assimilation (Stubbusch et al. 2024). The relatively stable growth pattern suggests that the strain possesses enzymatic machinery capable of degrading and assimilating these substrates efficiently, which is consistent with its origin from a fecal environment rich in heterogeneous organic matter. Similar metabolic flexibility has been reported for Bacillus spp., which are known to produce a broad spectrum of carbohydrate-active enzymes enabling the utilization of diverse polysaccharides (Chen and Yu 2023).

In contrast, sucrose and maltose supported only moderate growth, likely due to the requirement for extracellular or intracellular hydrolysis before these disaccharides can be metabolized, as indicated by Fujita 2009 and Liang et al. 2022. The additional enzymatic steps required may limit the rate of substrate uptake and delay entry into central metabolism, thereby reducing the overall growth rate. D-fructose, although a monosaccharide, showed relatively lower and more fluctuating growth, which may be attributed to differences in transport efficiency or regulatory effects on glycolytic flux. Previous studies have shown that fructose metabolism in Bacillus can be subject to specific regulatory controls distinct from glucose, potentially affecting growth efficiency under certain conditions (Ouhib-Jacobs et al. 2009).

When compared with other Bacillus species, the observed growth behavior of SLBD is consistent with previously reported patterns, where simple carbon sources such as glucose and glycerol promote rapid biomass formation, while more complex substrates result in slower but often more sustained growth (Ouhib-Jacobs et al. 2009). Importantly, the variation in growth kinetics among carbon sources reflects underlying metabolic regulation, particularly the balance between energy generation, biomass synthesis, and the expression of extracellular enzymes. In many Bacillus strains, conditions that support moderate growth rather than maximal biomass are often associated with enhanced production of hydrolytic enzymes, due to reduced CCR and increased nutrient-scavenging responses (Görke and Stülke 2008).

These findings demonstrate that carbon source selection plays a critical role in shaping the growth dynamics of *B. amyloliquefaciens* SLBD. While glycerol appears to be the most favorable substrate for biomass accumulation, alternative carbon sources such as inulin hydrolysate may offer advantages in terms of metabolic flexibility and potential enzyme production. This highlights the importance of considering not only growth performance but also metabolic regulation when optimizing fermentation conditions for hydrolytic enzyme production.

Specific growth rate

The specific growth rate (μ) of *Bacillus amyloliquefaciens* SLBD varied moderately across the tested carbon sources, ranging from approximately 0.167 to 0.179 h^{-1}, indicating relatively comparable

exponential growth kinetics under the different substrate conditions (Table 1). Among the substrates, sucrose and inulin hydrolysate exhibited slightly higher μ values (~ 0.179 h^{-1}), followed closely by D-glucose and D-fructose, while D-glycerol and maltose showed marginally lower growth rates (μ ≈ 0.167–0.169 h^{-1}). Despite these relatively small differences in μ, D-glycerol supported the highest biomass accumulation, as reflected by the maximum optical density achieved in the growth curve, indicating superior substrate utilization efficiency over extended cultivation. In contrast, fructose and maltose exhibited comparatively lower biomass formation, consistent with their less pronounced growth profiles.

Table 1
Kinetic growth curve of *Bacillus amyloliquefaciens* SLBSD under different carbon source

D-glycerol	**μ (h^{-1})**	**Doubling time (h)**	**Biomass (g/L)**
	0.169	**4.10**	**0.055**
D-glucose	0.173	4.00	0.039
Sucrose	0.179	3.87	0.030
D-fructose	0.177	3.92	0.033
Maltose	0.167	4.15	0.033
Inulin hydrolysate	0.179	3.87	0.034

These kinetic results are in good agreement with the growth curve patterns, where glycerol displayed sustained exponential growth and reached the highest final biomass, whereas fructose and maltose showed more gradual increases and lower overall cell density. The close alignment between μ values and growth profiles confirms that the exponential phase between approximately 5–15 h, represents the most metabolically active period for SLBD growth. This observation is consistent with Görke and Stülke 2008, who reported that glycerol is an effective carbon source for Bacillus due to its efficient assimilation into central metabolism and its relatively weak effect on carbon catabolite repression (CCR) compared to glucose.

The superior biomass yield observed with glycerol can be attributed to its metabolic entry point and regulatory characteristics, as reported by Yang et al. 2015. Glycerol is assimilated via glycerol kinase and converted into dihydroxyacetone phosphate (DHAP), directly feeding into central carbon metabolism without strongly triggering CCR. This allows sustained metabolic flux and prolonged growth, as observed in the growth curve. In contrast, glucose, although readily metabolizable, is a potent inducer of CCR in Bacillus spp., leading to repression of genes involved in alternative substrate utilization and, in some cases, limiting prolonged growth under batch conditions (Görke and Stülke 2008). This explains the rapid early growth followed by earlier plateau observed in glucose-containing cultures despite relatively comparable μ values.

The moderate growth rates observed for sucrose and inulin hydrolysate suggest that SLBD possesses enzymatic capabilities to utilize more complex carbohydrates, albeit with additional metabolic costs. This is a hallmark of *B. amyloliquefaciens*, which harbors a diverse repertoire of carbohydrate-active enzymes (CAZymes) (Niazi et al. 2014). Disaccharides such as sucrose and oligosaccharides present in inulin hydrolysate require prior hydrolysis before entering central metabolism, which may slightly reduce apparent growth efficiency compared to simpler substrates (Tian et al. 2011). Nevertheless, the relatively stable μ values combined with sustained biomass formation indicate that the strain is well adapted to complex substrates, consistent with its origin from fecal environments rich in heterogeneous organic matter. Similar metabolic flexibility has been reported for *Bacillus amyloliquefaciens* and related species, which produce diverse CAZymes to exploit a wide range of carbon sources (Niazi et al. 2014).

In contrast, the slightly lower growth rates and biomass accumulation observed with maltose and D-fructose highlight substrate-specific regulatory and transport limitations. Although both are metabolizable sugars, their uptake and catabolism in Bacillus may involve inducible systems or less efficient transport mechanisms, resulting in slower growth kinetics, as reported by Wen et al. 2021. Furthermore, fructose metabolism is subject to distinct regulatory pathways that may not support maximal glycolytic flux compared to glucose or glycerol. Overall, the variation in growth behavior across carbon sources reflects the interplay between substrate uptake efficiency, metabolic pathway integration, and global regulatory mechanisms such as CCR, as discussed in Zhang et al. 2025 and Jiang et al. 2021. These findings emphasize that carbon source selection not only influences biomass accumulation but also shapes the metabolic state of the cells, which is critical for downstream processes such as hydrolytic enzyme production.

Protease activity

The temporal profile of protease specific activity in *Bacillus amyloliquefaciens* SLBD showed a clear dependence on both incubation time and carbon source, with a general trend of low activity during the early growth phase followed by a pronounced increase during the late exponential to early stationary phase. Across all substrates, protease activity remained minimal during the lag (0–5 h) and early exponential phase (5–10 h), which is consistent with the prioritization of biomass formation over secondary metabolite production **(**Fig. 2**).** A marked increase in specific activity was observed between 12 and 24 h, coinciding with the transition from exponential to stationary phase identified in the growth curves. The highest protease activities were generally recorded around 24–30 h, after which activity either plateaued or declined, indicating enzyme instability or reduced secretion during the late stationary or decline phase. Earlier, Shah et al. 2025 reported that protease production by *B. amyloliquifaciens*. The finding also validates the temporal profile where protease production is triggered at the onset of the stationary phase as a response to nutrient depletion. In addition, Aguilar et al. 2019 reported the physiological switch in Bacillus where secondary metabolites and extracellular enzymes are prioritized only after the exponential growth phase.

Among the tested carbon sources, D-glycerol resulted in the highest protease specific activity, reaching a pronounced peak at approximately 30 h, which aligns with its superior growth performance (highest μ

and biomass). This suggests that glycerol not only supports rapid growth but also promotes efficient enzyme production, likely due to reduced carbon catabolite repression (CCR). In contrast, D-glucose exhibited moderate protease activity despite supporting relatively high growth rates, particularly during the early stages. This decoupling between growth and enzyme production is characteristic of CCR, where easily metabolizable sugars repress the expression of extracellular enzymes, including proteases, as cells prioritize energy-efficient pathways (Görke and Stülke 2008). Consequently, although glucose-supported cultures reached substantial biomass, their protease production was comparatively lower than glycerol.

Intermediate protease activities were observed for inulin hydrolysate, sucrose, and maltose, which generally peaked between 24 and 30 h. These substrates likely impose a mild metabolic burden due to the requirement for enzymatic hydrolysis prior to assimilation, which may delay growth but simultaneously induce extracellular enzyme production as part of a nutrient-scavenging response. This phenomenon is well documented in Bacillus spp., where complex or less readily metabolizable carbon sources alleviate CCR and promote the secretion of hydrolytic enzymes (Singh et al. 2008). The relatively stable and sustained protease activity observed with inulin hydrolysate further supports the metabolic adaptability of SLBD to complex substrates, consistent with its fecal origin.

In contrast, D-fructose showed comparatively lower and more fluctuating protease activity throughout the cultivation period, despite supporting moderate growth. This suggests that fructose metabolism in SLBD may not effectively induce protease expression, potentially due to differences in regulatory pathways or transport efficiency. Previous studies have indicated that different sugars can distinctly influence global regulatory networks, affecting not only growth but also enzyme secretion profiles (Zhina et al. 2021). Overall, the observed patterns highlight that protease production in *B. amyloliquefaciens* SLBD is growth-phase dependent and strongly modulated by carbon source, with optimal production occurring during the late exponential to early stationary phase under conditions that minimize CCR.

Taken together, the integration of growth kinetics and enzyme activity profiles indicates that the highest protease production does not necessarily coincide with the fastest growth, but rather with metabolic conditions that favor extracellular enzyme secretion. Glycerol emerges as the most favorable carbon source, providing both high biomass and elevated protease activity, while more complex substrates offer a balance between growth and enzyme induction. These findings emphasize the importance of carbon source selection in optimizing fermentation strategies for hydrolytic enzyme production.

Lipolytic activity

The lipolytic activity of *Bacillus amyloliquefaciens* SLBD exhibited a clear growth phase–dependent pattern, with minimal activity observed during the lag and early exponential phases (0–10 h), followed by a substantial increase during the mid to late exponential phase (10–24 h), and reaching peak activity in the early stationary phase (24–30 h) **(**Fig. 3**).** This trend closely mirrors the growth curve behavior, where maximal biomass accumulation transitions into a nutrient-limited state that typically triggers the secretion of extracellular enzymes. The delayed onset of lipase activity suggests that lipase production

in SLBD is not growth-associated but rather induced under conditions where cells shift from rapid proliferation to nutrient scavenging, a phenomenon commonly observed in Bacillus species (Gupta et al. 2004; Sharma et al. 2001).

Among the carbon sources tested, D-glycerol supported the highest lipolytic activity, with a pronounced peak around 30 h, consistent with its superior growth rate and biomass yield. This indicates that glycerol provides not only efficient carbon assimilation but also a metabolic environment conducive to lipase expression. It was earlier reported that glycerol was also reported to be the best sugar for enhancing lipase production in *B. safensis* VC-6. Unlike glucose, glycerol metabolism typically exerts weaker carbon catabolite repression (CCR), thereby allowing continued expression of extracellular enzymes even during active growth (Görke Stülke 2008). In contrast, D-glucose showed moderate lipase activity despite relatively strong growth performance during the early stages, suggesting partial repression of lipase synthesis due to CCR effects. This decoupling between biomass formation and enzyme production highlights the regulatory role of carbon source in controlling metabolic allocation.

Inulin hydrolysate also demonstrated relatively high lipolytic activity, second only to glycerol, with a steady increase throughout the cultivation period. This suggests that SLBD is capable of efficiently utilizing complex carbohydrate mixtures while simultaneously inducing enzyme production. Such behaviour is consistent with the ecological origin of the strain, where adaptation to complex substrates requires coordinated secretion of hydrolytic enzymes. Similarly, maltose and sucrose supported moderate lipase production, with activity peaking during the stationary phase, likely due to the requirement for prior hydrolysis before assimilation. These substrates may partially relieve CCR, thereby enhancing enzyme secretion compared to glucose (Singh et al. 2008).

In contrast, D-fructose resulted in the lowest and most fluctuating lipolytic activity, despite supporting moderate growth. This may be attributed to differences in metabolic regulation and substrate uptake efficiency, as fructose utilization in Bacillus is known to be governed by distinct regulatory pathways that may not strongly induce lipase expression (Zhina et al. 2021). Furthermore, the relatively stable but lower activity observed across fructose cultures suggests that this substrate does not effectively trigger the metabolic shift required for maximal extracellular enzyme production.

Overall, the lipolytic activity profile reinforces the conclusion that enzyme production in *B. amyloliquefaciens* SLBD is strongly influenced by both growth phase and carbon source. The highest lipase activity occurring during the transition to stationary phase indicates that nutrient limitation and metabolic stress are key drivers of enzyme secretion. Glycerol emerges as the most favorable carbon source, supporting both high biomass and enhanced lipolytic activity, while complex substrates such as inulin hydrolysate offer a balance between growth and enzyme induction. These findings are consistent with previous reports that highlight the importance of substrate selection in optimizing lipase production in *Bacillus* spp. (Gupta et al. 2004).

CMCase activity

The CMCase (carboxymethyl cellulase) activity of *Bacillus amyloliquefaciens* SLBD exhibited a distinct growth phase–dependent pattern, characterized by low activity during the lag and early exponential phases (0–10 h), followed by a sharp increase during the mid-exponential phase (10–20 h), and reaching maximum activity during the late exponential to early stationary phase (20–30 h) **(**Fig. 4**).** This trend is consistent with the growth curve, where rapid biomass accumulation transitions into a nutrient-limited state that triggers the secretion of extracellular hydrolytic enzymes. The delayed onset of CMCase activity indicates that cellulase production is largely non-growth-associated and is induced when cells shift toward substrate degradation and nutrient acquisition, a behavior commonly reported in Bacillus spp. and other cellulolytic bacteria (Singh et al. 2008; Lynd et al. 2002).

Among the tested carbon sources, inulin hydrolysate resulted in the highest CMCase activity, with a pronounced peak around 30 h, followed by sucrose, while glycerol, maltose, and D-fructose showed moderate levels of activity. In contrast, D-glucose consistently produced the lowest CMCase activity throughout the cultivation period. The superior performance of inulin hydrolysate can be attributed to its complex carbohydrate composition, which likely acts as an inducer for cellulase production. Complex substrates such as fructo-oligosaccharides require enzymatic degradation prior to assimilation, thereby stimulating the expression of carbohydrate-active enzymes, including cellulases. This observation aligns with previous studies indicating that cellulase production is strongly induced by polymeric or structurally complex carbon sources rather than simple sugars (Singh et al. 2008).

The relatively high CMCase activity observed in sucrose-containing cultures further supports the notion that disaccharides can partially induce cellulolytic systems, although to a lesser extent than more complex substrates. In contrast, the low cellulase activity in glucose-grown cultures is indicative of strong carbon catabolite repression (CCR), a well-established regulatory mechanism in Bacillus species that suppresses the expression of genes involved in the degradation of alternative carbon sources when a preferred substrate is available (Görke and Stülke 2008). This explains the discrepancy between relatively good growth performance in glucose and poor CMCase production, highlighting a decoupling between biomass formation and enzyme secretion. Moderate CMCase activity observed with glycerol suggests that this substrate does not strongly repress cellulase expression, allowing a balanced metabolic state that supports both growth and enzyme production. Similarly, maltose and D-fructose exhibited intermediate activity levels, likely reflecting differences in transport efficiency and regulatory control over carbohydrate metabolism. The overall pattern indicates that substrates requiring additional enzymatic processing tend to promote higher cellulase production, as cells activate extracellular degradation pathways to access utilizable sugars. This adaptive response is consistent with the ecological role of *Bacillus amyloliquefaciens*, which is frequently found in environments rich in complex organic matter and is known for its ability to produce diverse hydrolytic enzymes.

Altogether, CMCase activity in *B. amyloliquefaciens* SLBD is strongly influenced by both growth phase and carbon source, with maximal activity occurring during the late exponential to early stationary phase under conditions that favor enzyme induction rather than rapid growth. Inulin hydrolysate emerged as the most effective carbon source for cellulase production, while glucose exerted a repressive effect. These

findings reinforce the importance of carbon source selection in optimizing cellulolytic enzyme production and highlight the metabolic trade-off between growth efficiency and extracellular enzyme synthesis.

Enzyme purification

The purification profiles of protease, lipase, and cellulase from *Bacillus amyloliquefaciens* SLBD, when interpreted alongside SDS–PAGE analysis, demonstrate that multiple hydrolytic enzymes can be selectively recovered from a single extracellular supernatant through differential physicochemical partitioning (Fig. 5). This is because of the enzymes exhibited different physicochemical properties which regulated their unique behaviour during purification (Razali et al. 2021). As shown in the purification Table 2, all three enzymes exhibited a consistent increase in specific activity following ammonium sulfate precipitation and subsequent size exclusion chromatography (SEC), confirming progressive enrichment of catalytically active fractions. However, this enrichment was accompanied by a reduction in total protein and activity, reflecting the classical trade-off between purity and recovery in protein purification (Razali et al. 2021; Du et al. 2022). Importantly, the extent of enrichment and recovery differed among enzymes, indicating intrinsic differences in solubility, stability, and secretion behavior.

Table 2
Purification profile of hydrolytic enzymes of *Bacillus amyloliquefaciens* SLBD grew under their respected best carbon source

Enzyme	Step	Volume (mL)	Protein (mg/mL)	Total protein (mg)	Specific activity (U/mg)	Total activity (U)	Purification fold	Yield (%)
Protease	Crude	500	0.056	28.0	3.67	102.8	1.00	100
	60% AS	55	0.220	12.1	6.10	73.8	1.66	71.8
	SEC	70	0.095	6.65	9.80	65.2	2.67	63.4
Lipase	Crude	500	0.066	33.0	40.0	1320	1.00	100
	90% AS	50	0.170	8.50	75.0	637.5	1.88	48.3
	SEC	65	0.090	5.85	118.0	690.3	2.95	52.3
Cellulase	Crude	500	1.05	525	84	44,100	1.00	100
	80% AS	60	4.20	252	128	32,256	1.52	73.1
	SEC	75	0.083	125	172	21,500	2.05	48.8

*AS = Ammonium sulphate precipitation

A central mechanistic insight from this study is that ammonium sulfate precipitation serves as the key discriminatory step enabling separation of the three enzymes from the same supernatant. Despite

originating from a single extracellular mixture, protease, lipase, and cellulase were selectively enriched at different saturation levels—approximately 60% for protease, 80% for cellulase, and 90% for lipase. This differential precipitation arises from variations in protein surface hydrophobicity and charge, which govern solubility in high ionic strength environments (Wingfield 1998). Thus, rather than functioning solely as a concentration step, ammonium sulfate fractionation effectively splits the enzyme mixture into distinct functional fractions prior to chromatographic purification, as highlighted by Sultan et al. 2025. This explains how a uniform culture supernatant can be resolved into enzyme-specific pools using the same downstream workflow, providing a practical strategy for simultaneous multi-enzyme recovery.

For protease, precipitation at 60% saturation followed by SEC resulted in an increase in specific activity from 3.67 to 9.80 U mg^{-1}, although with a yield of 63%. SDS–PAGE analysis supports this **(**Fig. 5A**)**, showing a distinct band at ~ 35 kDa after AP and SEC, consistent with typical Bacillus proteases (Mahmoud et al. 2021). However, the persistence of faint additional bands indicates incomplete purification, with estimated purity of ~ 60–70%. This suggests co-precipitation of other proteins and possible autolytic degradation, which is common for extracellular proteases and likely contributes to activity loss during purification (Razali et al. 2021). Thus, while ammonium sulfate at 60% effectively enriches protease, its narrow precipitation window and structural instability limit recovery efficiency.

In contrast, lipase, which precipitated at a higher saturation (90%), exhibited a more favorable purification profile, with specific activity increasing from ~ 40 to 118 U mg^{-1} and retention of ~ 52.3% activity after SEC. SDS–PAGE reveals a prominent band at ~ 46 kDa with significantly reduced background, corresponding to an estimated purity of ~ 70–80% (Fig. 5B). The requirement for higher salt concentration indicates that lipase remains soluble at lower ionic strength, likely due to its hydrophobic interaction and stable tertiary fold (Sharma et al. 2001). This property enhances selective precipitation and contributes to improved downstream recovery. The relatively clean band after SEC further suggests that lipase benefits from both effective fractionation and structural resilience during purification.

Cellulase, enriched at ~ 80% ammonium sulfate saturation, displayed the highest purification fold (~ 2.05) and specific activity (172 U mg^{-1}), with moderate yield (48.8%). SDS–PAGE confirms a strong band at ~ 65 kDa with fewer contaminants compared to protease, indicating higher enrichment (estimated purity ~ 75–85%) **(**Fig. 5C**)**. The intermediate precipitation behavior reflects its larger, modular structure, often containing carbohydrate-binding domains that influence solubility and chromatographic behavior (Lynd et al. 2002). The selective enrichment of cellulase at 80% saturation highlights the effectiveness of stepwise precipitation in isolating enzymes with distinct structural features.

Importantly, the SDS–PAGE profiles also reveal that SEC alone is insufficient to achieve complete purity, as minor bands remain visible in all enzyme fractions. This indicates that while the combination of differential ammonium sulfate precipitation and SEC successfully resolves the three enzymes, additional purification steps (e.g., ion-exchange chromatography) are required for homogeneity (Sultan et al. 2025). Nevertheless, the current strategy achieves substantial enrichment and clearly demonstrates that

enzyme-specific fractionation can be achieved from a single extracellular pool without the need for separate cultivation processes.

When linked to upstream conditions, the role of carbon source becomes evident in shaping not only enzyme production but also purification behavior. Enzymes produced under optimal substrates—glycerol for protease and lipase, and complex carbohydrates for cellulase—are not only expressed at higher levels but may differ in folding, secretion state, and stability, influencing their precipitation profiles and chromatographic resolution (Görke and Stülke 2008). This reinforces the concept that upstream metabolic regulation and downstream separation are intrinsically connected, and that optimization of carbon source selection can directly enhance purification efficiency.

Overall, this study demonstrates that stepwise ammonium sulfate fractionation (60% → 80% → 90%) is a critical and effective strategy for resolving multiple extracellular enzymes from a single bacterial supernatant, enabling selective enrichment prior to SEC. The combined activity and SDS–PAGE data confirm successful recovery of protease (~ 35 kDa), lipase (~ 56 kDa), and cellulase (~ 70 kDa), although further purification is required for complete homogeneity. These findings provide a mechanistic and practical framework for multi-enzyme recovery systems and highlight the importance of integrating upstream cultivation strategies with downstream processing design.

Conclusions

Carbon source selection critically influences both growth and hydrolytic enzyme production in *Bacillus amyloliquefaciens* SLBD. Glycerol supported the highest biomass and enhanced protease and lipase production, while inulin hydrolysate was more effective for cellulase induction, reflecting a trade-off between growth and enzyme expression. Enzyme production peaked during the late exponential to early stationary phase, indicating regulation by nutrient limitation. Furthermore, multiple enzymes were successfully recovered from a single supernatant through differential ammonium sulfate precipitation followed by size exclusion chromatography, demonstrating a practical strategy for simultaneous multi-enzyme separation. However, additional purification is required for full homogeneity. Overall, integrating optimized fermentation conditions with efficient downstream processing provides a viable approach for cost-effective multi-enzyme production using locally sourced microbial strains.

Declarations

Acknowledgements

This research is funded by the Indonesian Endowment Fund for Education (LPDP) on behalf of the Indonesian Ministry of Higher Education, Science and Technology and managed under the EQUITY Program (Contract No: 59530/IT3.D10/PT.01.03/P/B/2025).

Author contributions

ET: Conceptualization, Methodology, Funding acquisition, Data curation, Formal analysis, Writing – original draft, Writing – review & editing, Supervision. RH: Investigation, Data curation, Data acquisition. HA, R.R: Investigation, Data curation, Data acquisition. MA: Investigation, Data acquisition. SW: Conceptualization, Funding acquisition, Writing – review & editing, Supervision. HD: Conceptualization, Funding acquisition, Writing – review & editing, Supervision. CB: Methodology, Funding acquisition, Writing – review & editing, Supervision. All authors and responsible authorities where the work was carried out have approved its publication.

Funding

The Indonesian Ministry of Higher Education, Science and Technology and managed under the EQUITY Program (Contract No: 59530/IT3.D10/PT.01.03/P/B/2025).

Data availability

All data supporting the findings of this study are available within the paper.

Declarations ethics approval

Not Applicable.

Consent to publish

All the authors agreed to publish this article.

Competing interests

The authors declare no competing interests.

References

1. Adeoyo OR (2025) Bioeconomic perspectives of bacterial and fungal hydrolytic enzymes: A review. Int J Sci Res Biol Sci 12:61–70. https://doi.org/10.26438/ijsrbs.v12i1.670
2. Aguilar JGDS, Castro RJSD, Sato HH (2019) Alkaline protease production by Bacillus licheniformis LBA 46 in a bench reactor: Effect of temperature and agitation. Braz J Chem Eng 36:615–625. https://doi.org/10.1590/0104-6632.20190362s20180014
3. Astuti RAW, Rahmani N, Zilda DS et al (2024) Prospects for primary design study of protease encoding genes for recombinant protease enzymes: A bibliographic and journal review. In: Lawang Sewu International Symposium on Health Sciences: Medical Laboratory Technology (LSISHS-MLT 2023). Atlantis Press, pp 5–15. https://doi.org/10.2991/978-94-6463-457-0_2
4. Bizzini A, Zhao C, Budin-Verneuil A et al (2010) Glycerol is metabolized in a complex and strain-dependent manner in *Enterococcus faecalis*. J Bacteriol 192:779–785. https://doi.org/10.1128/JB.00959-09

5. Brückner R, Titgemeyer F (2002) Carbon catabolite repression in bacteria: Choice of the carbon source and autoregulatory limitation of sugar utilization. FEMS Microbiol Lett 209:141–148. https://doi.org/10.1016/S0378-1097(02)00559-1
6. Budiman C, Razak RA, Unggit ARA et al (2022) Catalytic properties of caseinolytic protease subunit of *Plasmodium knowlesi* and its inhibition by a member of δ-lactone, hyptolide. Molecules 27:3787. https://doi.org/10.3390/molecules27123787
7. Chen YW, Yu YH (2023) Differential effects of *Bacillus subtilis* and *Bacillus licheniformis* fermented products on growth performance, intestinal morphology, intestinal antioxidant and barrier function gene expression, cecal microbiota community, and microbial carbohydrate-active enzyme composition in broilers. Poult Sci 102:102670. https://doi.org/10.1016/j.psj.2023.102670
8. Du M, Hou Z, Liu L et al (2022) Progress, applications, challenges and prospects of protein purification technology. Front Bioeng Biotechnol 10:1028691. https://doi.org/10.3389/fbioe.2022.1028691
9. Falkenberg F, Rahba J, Fischer D et al (2022) Biochemical characterization of a novel oxidatively stable, halotolerant, and high-alkaline subtilisin from *Alkalihalobacillus okhensis* Kh10-101T. FEBS Open Bio 12:1729–1746. https://doi.org/10.1002/2211-5463.13457
10. Fathi F, Kasra-Kermanshahi R, Moosavi-Nejad Z et al (2021) Partial purification, characterization and immobilization of a novel lipase from a native isolate of *Lactobacillus fermentum.* Iran J Microbiol 13:871–877. https://doi.org/10.18502/ijm.v13i6.8093
11. Fujita Y (2009) Carbon catabolite control of the metabolic network in *Bacillus subtilis*. Biosci Biotechnol Biochem 73:245–259. https://doi.org/10.1271/bbb.80479
12. Görke B, Stülke J (2008) Carbon catabolite repression in bacteria: Many ways to make the most out of nutrients. Nat Rev Microbiol 6:613–624. https://doi.org/10.1038/nrmicro1932
13. Gupta R, Gupta N, Rathi P (2004) Bacterial lipases: An overview of production, purification and biochemical properties. Appl Microbiol Biotechnol 64:763–781. https://doi.org/10.1007/s00253-004-1568-8
14. Hall BG, Acar H, Nandipati A et al (2014) Growth rates made easy. Mol Biol Evol 31:232–238. https://doi.org/10.1093/molbev/mst187
15. Imran M, Nazar M, Saif M et al (2016) Role of enzymes in animal nutrition: A review. PSM Vet Res 1:38–45.
16. Jiang W, Hernández Villamor D, Peng H et al (2021) Metabolic engineering strategies to enable microbial utilization of C1 feedstocks. Nat Chem Biol 17:845–855. https://doi.org/10.1038/s41589-021-00836-0
17. Kognou ALM, Chio C, Khatiwada JR et al (2023) Characterization of glucose isomerase-producing bacteria and optimization of fermentation conditions for producing glucose isomerase using biomass. Green Chem Eng 4:239–249. https://doi.org/10.1016/j.gce.2022.05.003
18. Kopp J, Slouka C, Ulonska S et al (2018) Impact of glycerol as carbon source onto specific sugar and inducer uptake rates and inclusion body productivity in *Escherichia coli* BL21(DE3).

Bioengineering 5:1. https://doi.org/10.3390/bioengineering5010001

19. Korajkic A, Wanjugi P, Brooks L et al (2019) Persistence and decay of fecal microbiota in aquatic habitats. Microbiol Mol Biol Rev 83:e00005-19. https://doi.org/10.1128/MMBR.00005-19
20. Kumar A, Dhiman S, Krishan B et al (2024) Microbial enzymes and major applications in the food industry: A concise review. Food Prod Process Nutr 6:85. https://doi.org/10.1186/s43014-024-00261-5
21. Laemmli UK (1970) Cleavage of structural proteins during the assembly of the head of bacteriophage T4. Nature 227:680–685. https://doi.org/10.1038/227680a0
22. Lee A, Cheng K-C, Liu J-R (2017) Isolation and characterization of a *Bacillus amyloliquefaciens* strain with zearalenone removal ability and its probiotic potential. PLoS One 12:e0182220. https://doi.org/10.1371/journal.pone.0182220
23. Liang J, van Kranenburg R, Bolhuis A, Leak DJ (2022) Removing carbon catabolite repression in *Parageobacillus thermoglucosidasius* DSM 2542. Front Microbiol 13:985465. https://doi.org/10.3389/fmicb.2022.985465
24. Lindang HU, Subbiah VK, Rodrigues KF et al (2021) Isolation, identification, and characterization of phosphate-solubilizing bacteria, *Paenibacillus* sp., from the soil of Danum Valley Tropical Rainforest, Sabah, Malaysia. Biodiversitas 22:4370–4378. https://doi.org/10.13057/biodiv/d221037
25. Lynd L, van Zyl W, Pretorius I (2002) Microbial cellulose utilization: Fundamentals and biotechnology. Microbiol Mol Biol Rev 66:506–577. https://doi.org/10.1128/MMBR.66.3.506-577.2002
26. Ma Q, Yi J, Tang Y et al (2024) Co-utilization of carbon sources in microorganisms for the bioproduction of chemicals. Biotechnol Adv 73:108380. https://doi.org/10.1016/j.biotechadv.2024.108380
27. Ma Q, Yi J, Tang Y et al (2024) Co-utilization of carbon sources in microorganisms for the bioproduction of chemicals. Biotechnol Adv 73:108380. https://doi.org/10.1016/j.biotechadv.2024.108380
28. Mahmoud A, Kotb E, Alqosaibi AI et al (2021) In vitro and in silico characterization of alkaline serine protease from *Bacillus subtilis* D9 recovered from Saudi Arabia. Heliyon 7:e08148. https://doi.org/10.1016/j.heliyon.2021.e08148
29. Meng Z, Li W, Huang G et al (2026) Advances in the regulatory mechanism of enzymes involved in soluble sugar metabolism in fruits. Plants (Basel) 15:138. https://doi.org/10.3390/plants15010138
30. Miller GL (1959) Use of dinitrosalicylic acid reagent for determination of reducing sugar. Anal Chem 31:426–428. https://doi.org/10.1021/ac60147a030
31. Niazi A, Manzoor S, Asari S et al (2014) Genome analysis of *Bacillus amyloliquefaciens* subsp. plantarum UCMB5113: A rhizobacterium that improves plant growth and stress management. PLoS One 9:e104651. https://doi.org/10.1371/journal.pone.0104651
32. Obeng EM, Adam SNN, Budiman C et al (2017) Lignocellulases: A review of emerging and developing enzymes, systems, and practices. Bioresour Bioprocess 4:16. https://doi.org/10.1186/s40643-017-0146-8

33. Ouhib-Jacobs O, Lindley ND, Schmitt P, Clavel T (2009) Fructose and glucose mediate enterotoxin production and anaerobic metabolism of *Bacillus cereus* ATCC 14579T. J Appl Microbiol 107:821–829. https://doi.org/10.1111/j.1365-2672.2009.04254.x
34. Pan S, Underhill SA, Hamm CW et al (2024) Glycerol metabolism impacts biofilm phenotypes and virulence in *Pseudomonas aeruginosa* via the Entner–Doudoroff pathway. mSphere 9:e00786-23. https://doi.org/10.1128/msphere.00786-23
35. Potprommanee L, Wang X-Q, Han Y-J et al (2017) Characterization of a thermophilic cellulase from *Geobacillus* sp. HTA426, an efficient cellulase producer on alkali-pretreated lignocellulosic biomass. PLoS One 12:e0175004. https://doi.org/10.1371/journal.pone.0175004
36. Razali R, Kumar V, Budiman C (2020) Structural insights into the enzymatic activity of cysteine protease bromelain of MD2 pineapple. Pak J Biol Sci 23:829–838. https://doi.org/10.3923/pjbs.2020.829.838
37. Razali R, Subbiah VK, Budiman C (2021) Technical data of heterologous expression and purification of SARS-CoV-2 proteases using *Escherichia coli* system. Data 6:99. https://doi.org/10.3390/data6090099
38. Shah TA, Li Z, Zhang A et al (2025) Production of alkaline protease from *Bacillus amyloliquefaciens* TAS-2 and optimizing fermentation conditions. Biocatal Biotransformation 43:496–509. https://doi.org/10.1080/10242422.2025.2527615
39. Sharma R, Chisti Y, Banerjee UC (2001) Production, purification, characterization, and applications of lipases. Biotechnol Adv 19:627–662. https://doi.org/10.1016/S0734-9750(01)00086-6
40. Shiddiq RHA, Budiman C, Asis H et al (2025) Morphological and biochemical characterization of a cellulose-degrading bacteria isolated from horse feces (*Equus caballus*). IOP Conf Ser Earth Environ Sci 1484:012036. https://doi.org/10.1088/1755-1315/1484/1/012036
41. Singh KD, Schmalisch MH, Stülke J et al (2008) Carbon catabolite repression in *Bacillus subtilis*: Quantitative analysis of repression exerted by different carbon sources. J Bacteriol 190:7275–7284. https://doi.org/10.1128/JB.00848-08
42. Sonnleitner E (2025) A comparative analysis: Molecular mechanisms of carbon catabolite repression in bacteria. Annu Rev Microbiol 79:241–262. https://doi.org/10.1146/annurev-micro-050624-031622
43. Stubbusch AKM, Keegstra JM, Schwartzman J et al (2024) Polysaccharide breakdown products drive degradation-dispersal cycles of foraging bacteria through changes in metabolism and motility. eLife 13:RP93855. https://doi.org/10.7554/eLife.93855.3
44. Sultan HM, Batool L, Hussain I et al (2025) An overview of protein purification strategies and applications. Medicinal and Medical Chemistry 2:98–112. https://doi.org/10.22034/MEDMEDCHEM.2025.531293.1037
45. Tian F, Inthanavong L, Karboune S (2011) Purification and characterization of levansucrases from *Bacillus amyloliquefaciens* in intra- and extracellular forms useful for the synthesis of levan and

fructooligosaccharides. Biosci Biotechnol Biochem 75:1929–1938. https://doi.org/10.1271/bbb.110315

46. Vershinina YS, Mitin IV, Garmay AV et al (2025) Simple and robust approach for determination of total protein content in plant samples. Foods 14:358. https://doi.org/10.3390/foods14030358
47. Wang Q, Qi Z, Fu W et al (2024) Research and prospects of enzymatic hydrolysis and microbial fermentation technologies in protein raw materials for aquatic feed. Fermentation 10:648. https://doi.org/10.3390/fermentation10120648
48. Wen J, Zhao X, Si F, Qi G (2021) Surfactin, a quorum sensing signal molecule, globally affects the carbon metabolism in *Bacillus amyloliquefaciens.* Metab Eng Commun 12:e00174. https://doi.org/10.1016/j.mec.2021.e00174
49. Wingfield P (1998) Protein precipitation using ammonium sulfate. Curr Protoc Protein Sci 13:1–10. https://doi.org/10.1002/0471140864.psa03fs13
50. Yahya NA, Fazal BZ, Razali R et al (2025) Screening and characterization of thermostable lipases-producing bacteria from Sabah hot springs. Malays J Microbiol 21:311–322. https://doi.org/10.21161/mjm.230248
51. Yang T, Rao Z, Zhang X et al (2015) Enhanced 2,3-butanediol production from biodiesel-derived glycerol by engineering of cofactor regeneration and manipulating carbon flux in *Bacillus amyloliquefaciens.* Microb Cell Fact 14:122. https://doi.org/10.1186/s12934-015-0317-2
52. Zhang C, Zhao Y, Li Z et al (2022) Molecular mechanism of GylR-mediated regulation of glycerol metabolism in *Streptomyces clavuligerus* NRRL 3585. Front Microbiol 13:1078293. https://doi.org/10.3389/fmicb.2022.1078293
53. Zhang J, Fang H, Du G et al (2025) Metabolic regulation and engineering strategies of carbon and nitrogen metabolism in *Escherichia coli.* ACS Synth Biol 14:1367–1380. https://doi.org/10.1021/acssynbio.5c00039
54. Zhina Q, Aqeel S, Harindintwali JD et al (2021) Engineering *Bacillus subtilis* for the production of high fructose syrup: Opportunities and prospects. Int J Environ Agric Biotechnol 6:101–109. https://doi.org/10.22161/ijeab.62.10

Figures

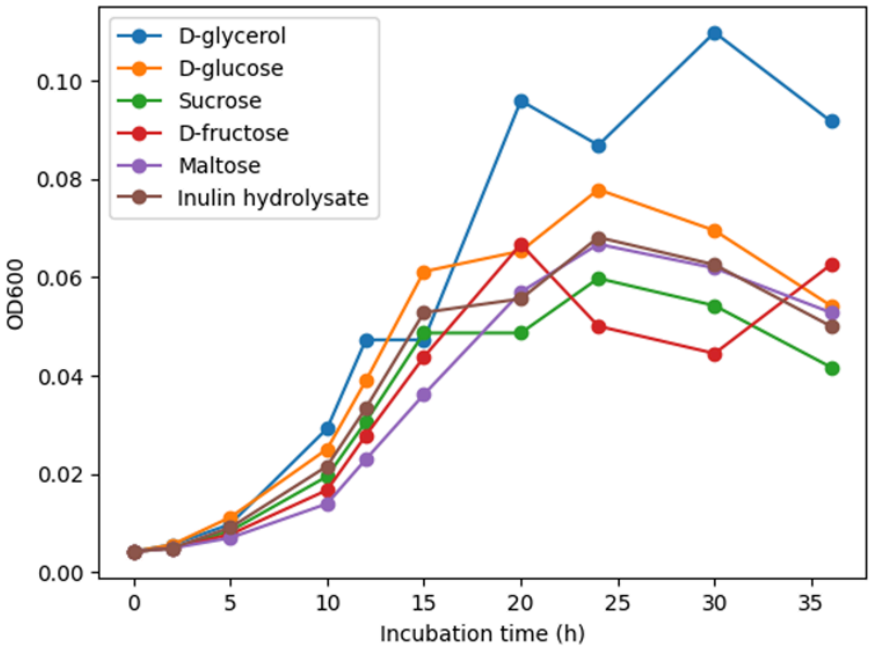


Figure 1

Figure 1

Growth curve of *B. amyloliquefaciens* SLBD under different carbonsources

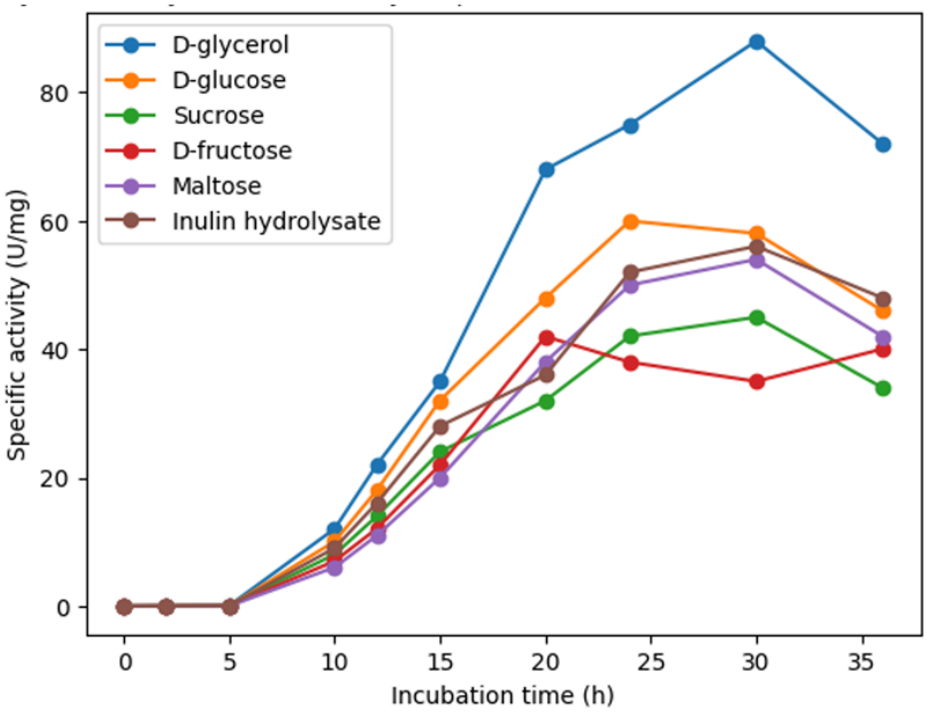


Figure 2

Figure 2

Protease activity of *B. amyloliquifaciens* SLBD during the growth under different carbon source

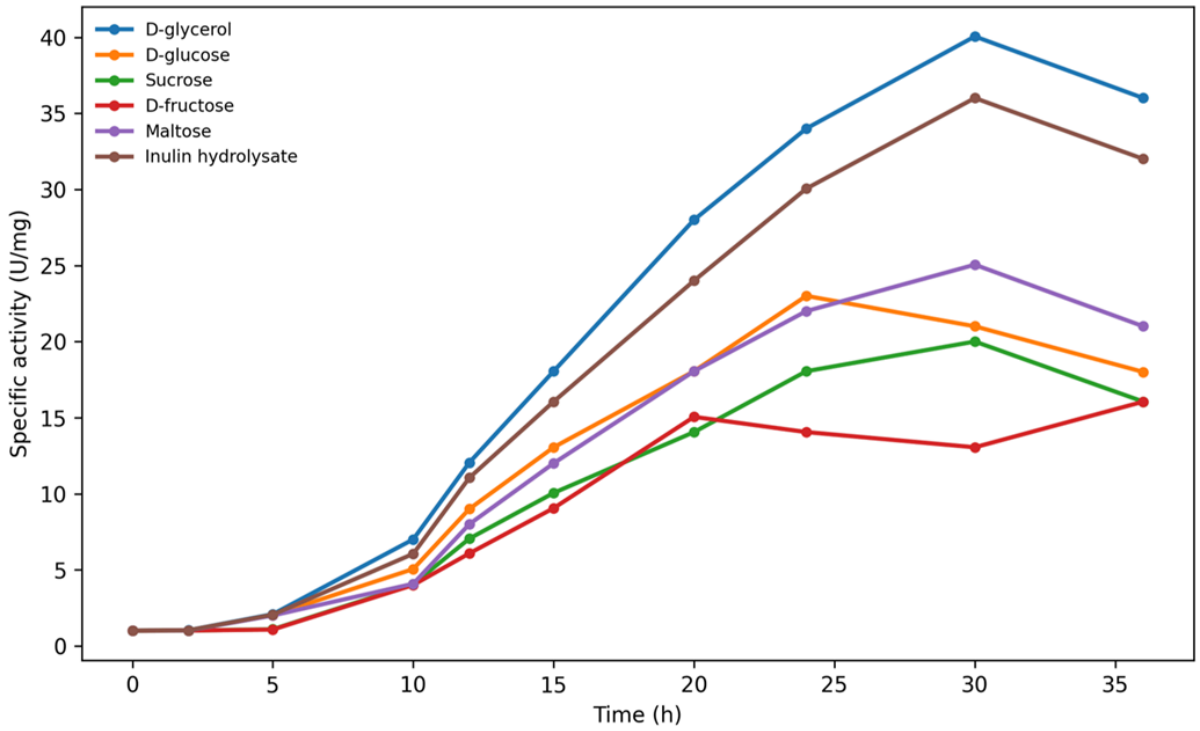


Figure 3

Figure 3

Lipolytic activity of *B. amyloliquifaciens* SLBD during the growth under different carbon source

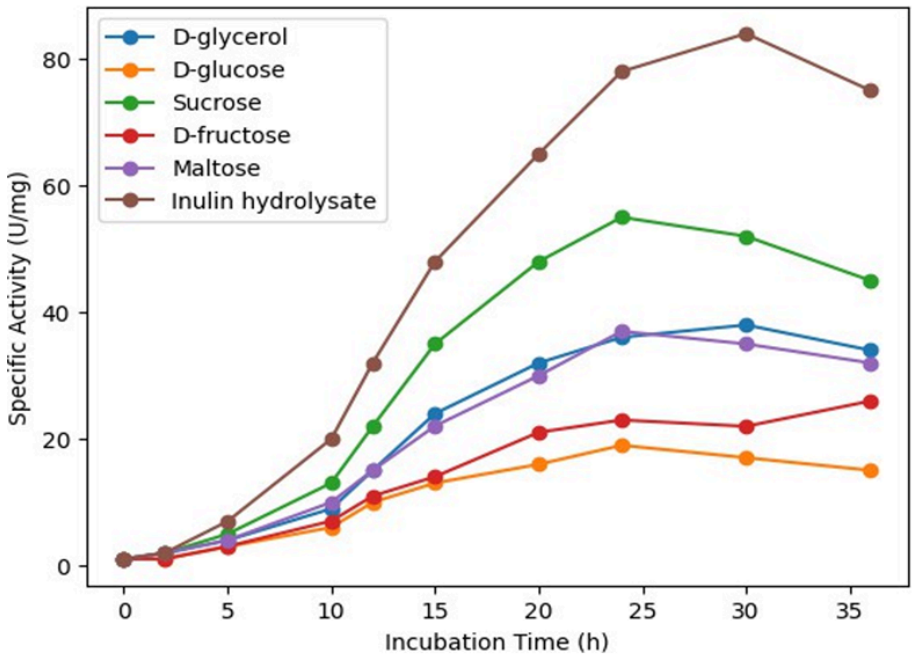


Figure 4

Figure 4

CMCase activity of *B. amyloliquifaciens* SLBD during the growth under different carbon source

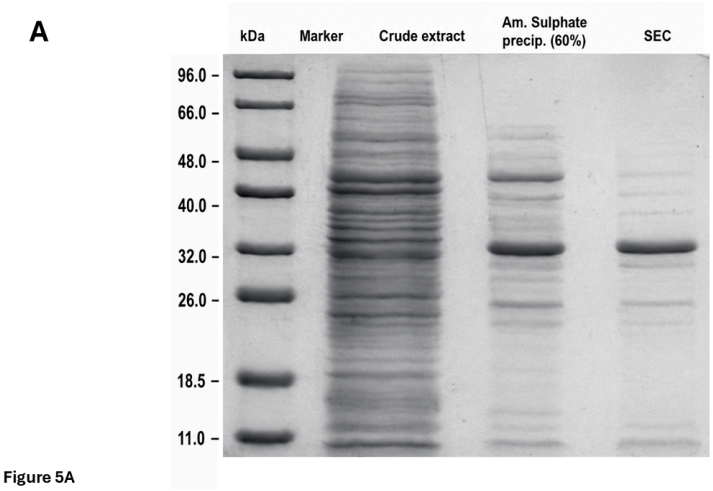


Figure 5A

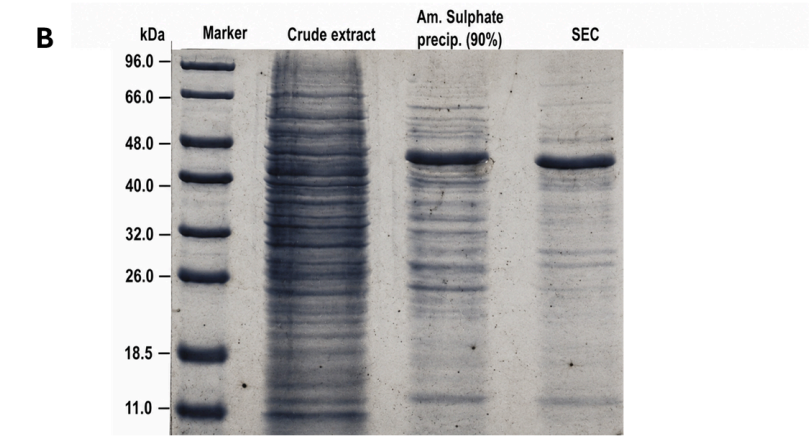


Figure 5B

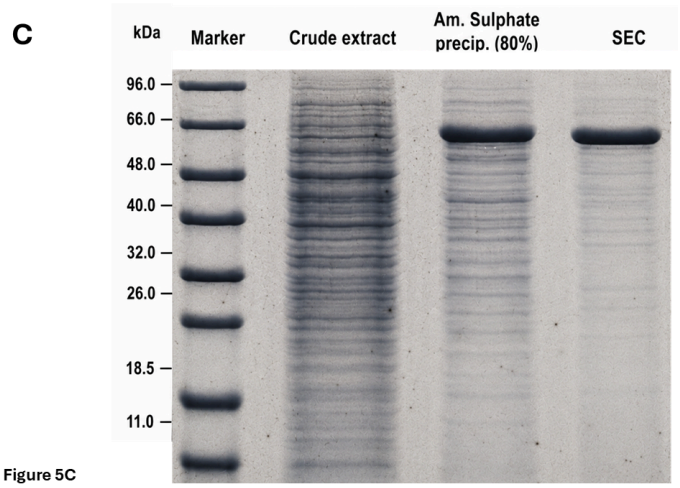


Figure 5C

Figure 5

SDS–PAGE analysis of protease purification at different purification steps for protease (A), lipase (B) and cellulases (C). Lane M, molecular weight marker (11–96 kDa); Lane 1, crude extracellular protein extract showing multiple protein bands; Lane 2, ammonium sulfate (AS) precipitated fraction, Lane 3, size-exclusion chromatography (SEC) fractions.